



# Climate sensitivity of high- and low-elevation *Larix decidua* MXD chronologies from the Tatra Mountains

Lara Klippel<sup>a,\*</sup>, Ulf Büntgen<sup>b,c,d,e</sup>, Oliver Konter<sup>a</sup>, Tomáš Kyncl<sup>f</sup>, Jan Esper<sup>a</sup>

<sup>a</sup> Department of Geography, Johannes Gutenberg University, Mainz, Germany

<sup>b</sup> Department of Geography, University of Cambridge, United Kingdom

<sup>c</sup> Swiss Federal Research Institute for Forest, Snow, and Landscape (WSL), Birmensdorf, Switzerland

<sup>d</sup> Global Change Research Institute of the Czech Academy of Sciences (CzechGlobe), 603 00 Brno, Czech Republic

<sup>e</sup> Department of Geography, Faculty of Science, Masaryk University, 613 00 Brno, Czech Republic

<sup>f</sup> Moravian Dendro-Labor, Brno, Czech Republic

## ARTICLE INFO

### Keywords:

Dendroclimatology  
Eastern Europe  
Maximum latewood density  
Slovakia  
Climate reconstruction

## ABSTRACT

Maximum latewood density (MXD) measurements from high-elevation/-latitude sites are an important proxy for summer temperature reconstructions. Here, we present 201 MXD series from living larch (*Larix decidua* Mill.) trees that were growing at around 850 and 1450 m a.s.l. in the Slovakian Tatra Mountains, together with 56 MXD series from historical timbers of the same species and region. We explore the climate signal at the high- and low-elevation sites and assess the effects of varying temperature and precipitation regimes on MXD formation. Ranging from spring temperature to summer precipitation, the elevation-specific climate sensitivity suggests that the MXD measurements from living and relict sources should not be merged for paleoclimatic studies. This finding emphasizes the challenge of attributing a predominant climate factor that controls wood formation across a wide range of historical constructions. A better understanding of the ‘true’ climate signal requires more samples during the period of overlap between the living and historical trees.

## 1. Introduction

Information about annual to centennial scale climate dynamics relies on indirect climate recorders, so-called natural proxy archives that capture climate information in their physical and chemical properties due to a lack of reliable instrumental precipitation and temperature measurements prior to the 19th century (Böhm et al., 2009). Proxy-derived, high-resolution climate reconstructions over the Common Era (CE), especially the past millennium, are crucial for placing the ongoing recent warming (Crutzen, 2002) in a long-term context of natural climate variability (Büntgen et al., 2011), and to assess whether the 0.8–1.2 °C warming since 1880 (IPCC, 2018), due to increasing concentrations of atmospheric greenhouse gases, is unprecedented compared to past climatic changes (Morice et al., 2012). The current understanding of annually resolved long-term European temperature variations derived from tree-rings relies on a handful of (near) millennium-long temperature sensitive tree-ring records from high-elevation tree line sites in the Alps (Büntgen et al., 2005, 2006b; Büntgen et al., 2011), Carpathians (Popa and Kern, 2009), Pindus (Esper et al., 2019; Klippel et al., 2018), Pyrenees (Büntgen et al., 2008, 2017;

Dorado Liñán et al., 2012), and Tatra (Büntgen et al., 2013), and from the northern tree line sites in Scandinavia (Esper et al., 2012; Gunnarson et al., 2011; Linderholm and Gunnarson, 2019; Melvin et al., 2013; Zhang et al., 2015a), and Scotland (Rydval et al., 2017). More than half of these records are maximum latewood density (MXD) or blue intensity (BI) based, whereas particularly in eastern Europe, records rely on the more commonly used dendrochronological parameter tree-ring width (TRW).

Compared to TRW, MXD contains an enhanced temperature signal (Wilson et al., 2016) and climatic information over longer growing seasons (Büntgen et al., 2007). It is less influenced by biological memory effects, producing chronologies with autocorrelation structures that are more similar to instrumental temperature data (Esper et al., 2015). Due to the reduced biological persistence, MXD is more suitable to detect abrupt inter-annual cooling events caused by volcanic eruptions (Esper et al., 2013; Schneider et al., 2015) or by severe defoliation events after insect outbreaks (Esper et al., 2007).

These properties clearly indicate the need to expand the network of multi-centennial-long MXD chronologies towards eastern Europe, where great potential is given in the Romanian Carpathian Mountains

\* Corresponding author.

E-mail address: [L.Klippel@geo.uni-mainz.de](mailto:L.Klippel@geo.uni-mainz.de) (L. Klippel).

<https://doi.org/10.1016/j.dendro.2020.125674>

Received 9 July 2019; Received in revised form 1 February 2020; Accepted 10 February 2020

Available online 11 February 2020

1125-7865/ © 2020 Elsevier GmbH. All rights reserved.

(Popa and Kern, 2009) and the Polish and Slovakian Tatra Mountains (Büntgen et al., 2013) with TRW chronologies covering the periods 1163–2005 and 1040–2011, respectively. Previous dendroclimatological analyses of *Larix decidua* and *Picea abies* MXD chronologies for the last 400 years show that MXD is highly suitable for temperature reconstruction in eastern Europe (Büntgen et al., 2007; Kaczka et al., 2018).

An indispensable step before assembling long tree-ring chronologies is the appropriate combination of living and historical timbers (Teigel et al., 2010). This includes the extension of the growth spectra of historical timbers with living trees from a similar growth environment. The so called data homogeneity between living and historical samples (Esper et al., 2016), permits the transfer of the recent growth-climate relationships into the past (Fritts, 1976). Ignoring the criterion and combination of different micro-sites (Düthorn et al., 2013), samples from different elevations (Zhang et al., 2015b) or slope expositions (Hartl-Meier et al., 2015) leads potentially to a pooling of samples with a different climate forcing that do not match signals retained in historical samples.

Thus here, we (1) introduce new MXD measurements from both, high-elevation and low-elevation *Larix decidua* sites in the High and Low Tatra Mountains and (2) assess inherent climate responses as a function of site elevation. Finally, we discuss the abilities of a potential usage of MXD to establish a millennium-long temperature reconstruction for eastern Europe by extending the chronology with historical samples.

## 2. Material and methods

### 2.1. Sampling site, tree-ring data and chronology development

All *Larix decidua* Mill. samples origin from the Greater Slovakian Tatra region with differences in site elevation. The high-elevation site is located at Dolina Mengusovska (1450 m a.s.l.; 49.14 N/20.07 E) in the Slovakian High Tatras, near the highest range of the Carpathian arc. The low-elevation site is situated south of the high-elevation site and close to the village Vernar (850 m a.s.l.; 48.93 N/20.29 E) in the Low Tatras (Fig. 1a). The sites differ geologically, as the High Tatra Mountains were formed by granites containing intrusions of metamorphic rocks (Burda et al., 2013; Gaweda, 2008), whereas the Low Tatra Mountains near Vernar are composed of Triassic sandstones, limestones and dolomites (Földvary, 1988). Historical material origins from beams of houses, churches and castles enclosed by these ranges. In different field campaigns in 2004, 2011, 2012, and 2017, a total of 114 high-elevation, 126 low-elevation and 263 historical TRW measurements were established and different subsets previously published by Büntgen et al. (2013) to establish a nearly millennium-long May-June temperature reconstruction for Eastern Europe, in Büntgen et al. (2007) to assess growth responses to climate in a multi-species tree-ring network, in Konter et al. (2015a) to test for spatiotemporal variations in the climatic response in *Larix decidua* TRW samples, and in Konter et al. (2015b) to verify the absence of larch budmoth outbreaks.

MXD measurements developed in this study base on a subset of the TRW samples. Only a little fraction could be processed for density measurements, because previous treatments of the cores, e.g. the preparation of the surface with a microtome and the fixation on wooden holders, caused damages and a general fragileness. MXD measurements were derived from high-precision X-ray radiodensitometry using the DENDRO2003 setup from Walesch Electronic. The cores were prepared according to standard dendrochronological techniques (Lenz et al., 1976; Schweingruber et al., 1978). To extract resins and other chemical or biochemical compounds, samples were treated 34 h with alcohol in a Soxhlet and 24 h in a water bath. Each sample was split in 1–3 cm long sections and 2 mm laths from these sections were cut perpendicular to the tracheid's longitudinal axis using a twin blade saw. The laths and a five-stepped cellulose acetate calibration wedge were exposed 14 min

to X-rays. Depth levels of the calibration wedge return reference grey levels and comparison with the grey-levels from the wood, enables estimates of the wood density. The high-elevation MXD measurements were merged with existing MXD data from Dolina Mengusovska of 2004 (Büntgen et al., 2007) and accessed via the ITRDB (<https://www.ncdc.noaa.gov/paleo-search/>; Grissino-Mayer and Fritts, 1997), which were developed in the same manner.

To remove non-climatic, age-related trends from the raw measurement MXD series, two cubic spline detrendings with a 50 % frequency-response cutoff equal to 10 years (10SP) and 100 years (100SP) were applied to retrain climate information at annual to multi-decadal timescales (Cook and Peters, 1981) using ARSTAN (Cook and Krusic, 2016). Prior to calculating residuals, all series were power-transformed (Cook and Peters, 1997), and the resulting site chronologies were variance stabilized according to Frank et al. (2007) to avoid bias from changes in sample replication and inter-series correlation. The strength of the common signal was estimated considering the expressed population signal (EPS; Wigley et al., 1984) and inter-series correlations (Rbar) calculated over 30-year periods with 15 years of overlap. Coherency between the high- and low-elevation MXD site chronologies, and the pooled chronology including all historical samples, was tested by calculating Pearson's correlation coefficients in 31-year moving windows over the chronologies' common periods. Over the period of overlap between historical and living material, this analysis was repeated using individual measurements and TRW data. The establishment of regional curves (RC), empirically defined as biological age stand curves (Briffa et al., 1992), and the comparison of absolute MXD values permits further inter-site comparison (Esper et al., 2003).

MXD measurements comprise a total of 111 high-elevation and 90 low-elevation samples (Fig. A.1 and Fig. 2d). The high- and low-elevation site chronologies cover the period 1676–2012 and 1745–2017 ( $n > 5$ ), respectively (Fig. 2a-b). Corresponding Rbar values of 0.45 and 0.33, and EPS values of 0.96 and 0.94, indicate strong intra-site coherency of the individual trees and suggest the mean chronologies contain some environmental information (Fig. 2e). With only 56 historical series over the period 1032–1853, and only exceeding  $n > 5$  samples in the intervals 1162–1315 and 1355–1600, Rbar values of 0.16 and an EPS of 0.57, signal strength and sample replication are very limited (Fig. 2c-e and Fig. A.1). Over the period 1500–1853 Rbar and EPS values were 0.16 and 0.39, respectively.

### 2.2. Climate and climate signal detection

During the growing season from April to September (Büntgen et al., 2007), weather and atmospheric settings in Slovakia develop under the influence of cyclonic and anti-cyclonic synoptic patterns associated with the strength of the westerlies (Niedzwiedz, 1992). Thermic and hydroclimatic conditions at the tree sites are additionally modulated by topography, causing a decrease of temperature with increasing elevation, and luv- and lee effects in the distribution of precipitation (Barry, 2008). Mean annual temperature and precipitation from 1961 to 1990 at the Poprad station (49.07 N and 20.25E, 695 m a.s.l.; Fig. 1) are 5.8 °C and 578 mm, respectively (Fig. 1). For MXD calibration, we used climate data from this meteorological station, which is reaching back to 1951.

The high- and low-elevation 100SP chronologies were correlated against monthly and seasonal temperature and precipitation data from previous-year August to current-year September, and the May-June seasonal mean. By calculating residuals from 10-year cubic smoothing splines, the instrumental data were additionally high-pass filtered for calibration against the 10SP chronologies. Spatial correlation analyses were performed between the high- and low-elevation 100SP MXD chronologies and 0.5° gridded CRU TS4.01 (Harris, 2015) climate data for the period 1951–2012 and the extended period 1901–2016 to assess climate signal strength and explore potential temporal changes. All meteorological data and correlation maps were retrieved from the

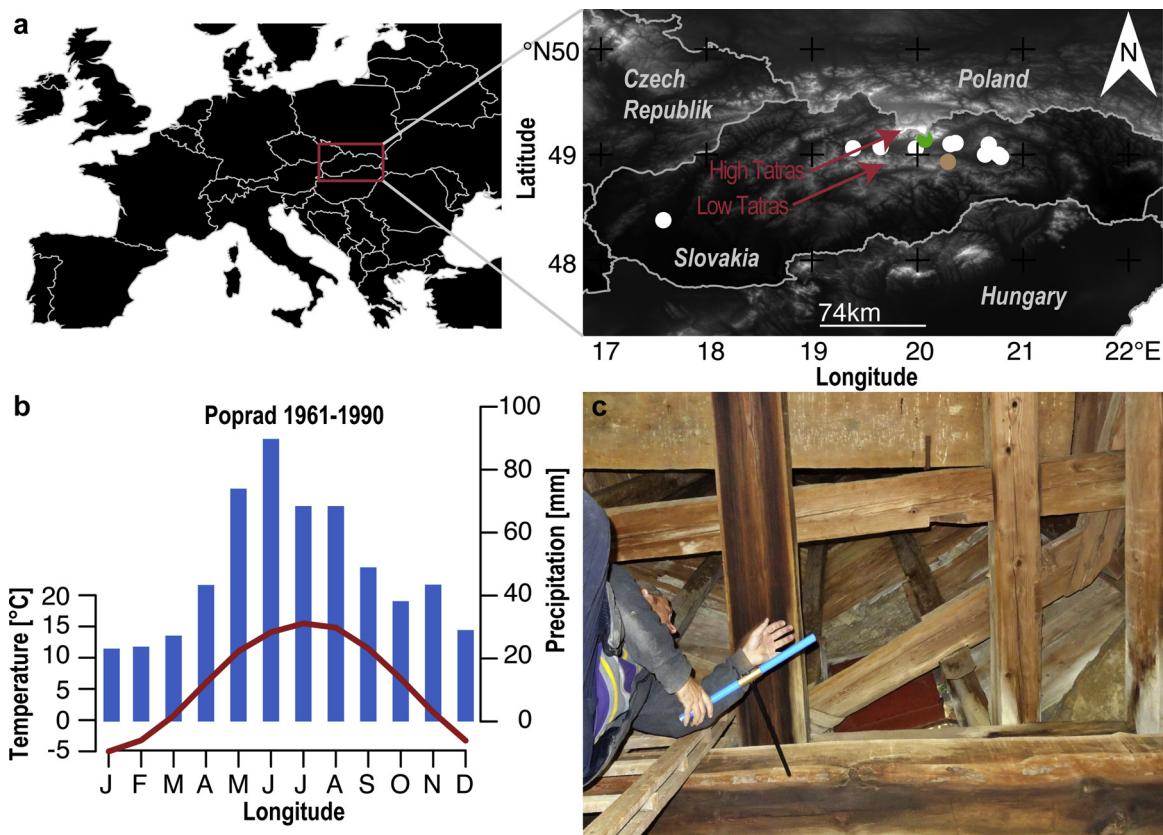


**Fig. 1.** a Location of the living tree high-elevation (green) and low-elevation (brown) sites, and historical (white) sampling locations within the area of the Tatra Mountains in Slovakia. b Climate diagram of the meteorological station in Poprad (49.07 N, 20.25E, 695 m a.s.l.), and c picture demonstrating the sampling of historical material in a church.

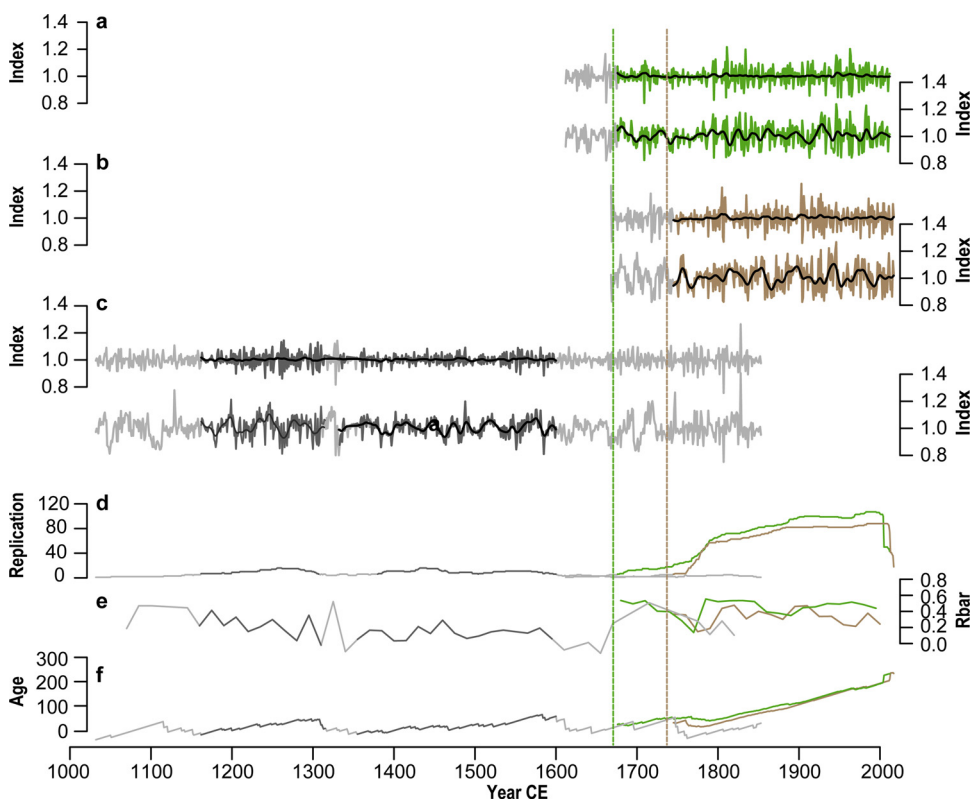


**Fig. 2.** Tatra MXD chronologies. a-b, 10SP (upper) and 100SP (lower) *Larix decidua* MXD chronologies from high (green) and low (brown) elevation sites, together with 15-year low-pass filters (black). Light grey lines indicate the period when sample replication is  $\leq 5$ . c, Same as in a-b, but for the historical material chronologies (dark and light grey). d, Sample size curves of the high, low, and historical chronologies. e, Rbar statistics of the raw MXD series (calculated over 30 years lagged by 15 years), and f, the corresponding mean age curves. The vertical dashed lines in 1680 CE (green) and 1730 CE (brown) indicate when EPS passes the 0.85 threshold in the high- and low-elevation raw chronologies, respectively.

Royal Netherlands Meteorological Institute's (KNMI) Climate Explorer (<https://climexp.knmi.nl>; Trouet and van Oldenborgh, 2013). The stability of climate/growth relationships were assessed for the most important month/season by iteratively modifying the tree-ring chronologies' sample replication to estimate effects on earlier, less replicated chronology periods. Multiple Pearson correlation coefficients were derived from the calibration of 2000 sub-sample high-elevation 100SP and 10SP chronologies against May-June temperatures, and sub-sample low-elevation 100SP and 10SP chronologies against July precipitation over the period 1951–2012. The tree-ring chronologies were developed using 5, 10, ..., 35 MXD series randomly drawn 2000 times from the population of 43 (high-elevation) and 69 (low-elevation), respectively that cover the entire calibration period.

### 3. Results

#### 3.1. Site characteristics

The 100SP chronologies reflect environmental changes at inter-annual to multi-decadal, and the 10SP chronologies at inter-annual timescales (Fig. 2a-c). Despite the application of a variance stabilization procedure (Frank et al., 2007), all chronologies are characterized by heterogeneous variance structures with periods of inflated and reduced variability. Mean segment length (MSL) is 200 years in the high-elevation and 206 years in low-elevation site, and tree ages increase towards present in both chronologies. The pool of historical samples is younger with a MSL of 94 years and ages ranging from 24 to 210 years, which guarantees a heterogeneous age structure through time (Figs. 2f and 3a; Esper et al., 2016). The RC's of the low-elevation site and historical samples overlap, whereas density in the high-elevation samples is at all age stages at a lower level (Fig. 3b). For the first 150 years of growth, average MXD is 0.89 g/cm<sup>3</sup> in high-elevation, 0.95 g/cm<sup>3</sup> in low-elevation and 0.98 g/cm<sup>3</sup> in historical trees (Fig. 3c). The absence of inter-site correlations over the common period of overlap 1676–2012 with  $r = -0.08$  between the 100SP high- and low-elevation chronologies ( $r = 0.1$  between 10SP chronologies and  $r = -0.11$  between 100SP plus additionally 10-year smoothed chronologies) points to substantial site-specific growth variations at high-to-low frequent scales as well as potential discrepancies to link historical samples with both site chronologies (see below).

#### 3.2. Climate growth relationships

The high- and low-elevation site chronologies contain inconsistent but distinct climate signals (Fig. 4). The high-elevation 10SP chronology strongly correlates with May-June temperatures ( $r = 0.68$ ,  $p < 0.001$ ), whereas the correlations are significantly lower for the 100SP chronology ( $r = 0.54$ ,  $p < 0.01$ ), indicating a stronger proxy/temperature coherency at inter-annual time scales. Significant correlations appear also in the month of September (10SP  $r = 0.42$ ,  $p < 0.01$  and 100SP  $r = 0.34$ ,  $p < 0.05$ ). The low-elevation 100SP chronology correlates significantly with March temperatures ( $r = 0.39$ ,  $p < 0.01$ )

and July precipitation ( $r = 0.44$ ,  $p < 0.001$ ). Here, the correlations are insignificantly lower for high-frequency, the 10SP chronology ( $r = 0.37$ ,  $p < 0.01$  and  $r = 0.43$ ,  $p < 0.001$ ). At the high-elevation site, however, substantial influences of March temperatures and July precipitation are absent, and vice versa, at the low-elevation site temperatures in May-June have no significant impact on latewood growth. For both sites, the months of the previous year summer to winter do not significantly influence density formation.

The recalculation of 2000 subset 100SP and 10SP chronologies from the high-elevation site, and their correlation with May-June temperature, shows that the signal is robust down to a replication of five series (Fig. 4b). The mean correlation with a random subset of five 100SP detrended series is  $r = 0.55$  ( $p < 0.01$ ) and  $r = 0.65$  ( $p < 0.001$ ) for a random subset of five 10SP detrended series. The absolute values range between 0.38–0.66 (100SP) and 0.51–0.75 (10SP), respectively. The same exercise using the 100SP and 10SP low-elevation chronologies and July temperature reveals that a robust growth/climate relationship at the lower elevation site requires high sample replications. Here, 20 series are needed to reach a signal strength passing the  $p < 0.05$  threshold.

Significant correlations  $r > 0.4$  between the high-elevation 100SP chronology and gridded May-June temperatures extend from Poland to Serbia in a north/south direction and from eastern Germany to western Ukraine in east/west direction (Fig. 5a). Correlations over central Germany, Latvia, Greece, Italy and Bulgaria are weaker, but still significant. Positive correlations between the low-elevation 100SP chronology and March temperatures cover roughly the same spatial domain, though values  $r > 0.4$  appear only close to the study site and rapidly decrease to  $r = 0.2$ – $0.3$  in neighboring countries (Fig. 5b). Strong positive correlations between the 100SP low-elevation chronology and July precipitation appear east of the study region, whereas the relationship completely disappears west of the study site (Fig. 5c). Considering the extended 1901–2016 period for calibration, the correlation fields are slightly weaker, particularly between the 100SP low-elevation chronology and March temperature (Fig. A.2), pointing to a weaker growth/climate relationship or potential biases in the early instrumental measurement data.

#### 3.3. Data homogeneity

Offsets in the absolute density values, low inter-site correlations at varying frequencies, and changing climate responses indicate substantial inter-site inhomogeneities at multiple timescales, and imply that a successful combination of the historical material with high- and low-elevation living tree populations is challenging. This result is confirmed by moving window correlations between the living chronologies and the historical chronology (Fig. 6). Over the common period of overlap ( $n > 3$  historical samples), coherence between the high-elevation chronology and the historical chronology is low ( $r = 0.02$ ) but higher ( $r = 0.46$ ) between the low-elevation chronology and the historical chronology. However, the validity of the comparison is very limited due to a low replication of  $n < 5$  samples. Comparison of the

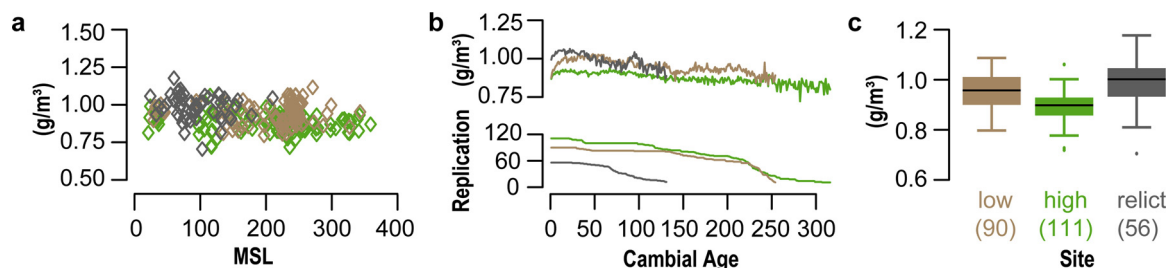


**Fig. 3.** MXD characteristics of high-elevation (green), low-elevation (brown) and historical (grey) larch trees. a, Mean MXD versus mean segment length. b, Regional curves and replication curves (> 10 series) of the high, low, and historical samples. c, Box plots of average MXD values over the first 150 years of tree growth. Numbers indicate sample replication.

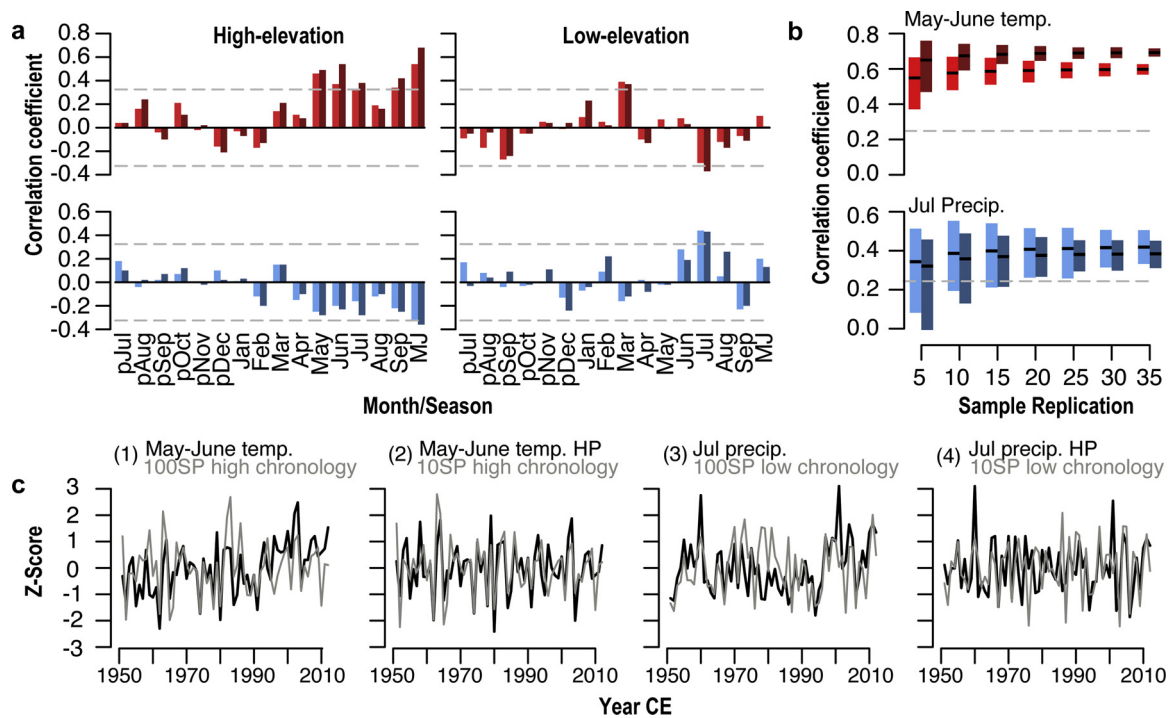


**Fig. 4.** Correlation coefficients of a, MXD high-elevation and low-elevation chronologies against monthly and seasonal temperatures (red) and precipitation (blue) from the Poprad meteorological station for the 1951-2012 period. Light colors refer to 100SP proxy and instrumental data and dark colors to 10SP and 10-year HP instrumental data. Dashed lines indicate  $p < 0.01$ . b Multiple correlation coefficients from calibrating 2000 100SP and 10SP high-elevation (low-elevation in the lower panel) sub-sample chronologies against May-June temperatures (July precipitation) from 1951-2012. The 100SP and 10SP chronologies were established randomly by resampling 5 to 35 MXD series from a population of 43 (69) living tree-ring series covering the calibration period (see methods). Dashed lines indicate  $p < 0.05$ . c, Z-scores of (1) instrumental May-June temperatures (black) and 100SP high-elevation chronology (grey) (2) instrumental 10-year HP May-June temperatures and 10SP high-elevation chronology, (3) instrumental July precipitation and 100SP low-elevation chronology and (4) instrumental 10-year HP July-precipitation and 10SP low-elevation chronology.

high- and low-elevation chronologies with the five historical MXD series reinforces this trend, with higher correlation coefficients for the low-elevation/historical comparison (ranging between  $r = 0.15-0.58$ ) and lower ( $r = -0.04-0.18$ ) for the high-elevation/historical comparison (Fig. A.3.).

#### 4. Discussion

##### 4.1. Altitudinal differences in growth/climate responses of MXD

Absolute density values in living larch samples decrease with an increasing altitude, which is in line with a previous study elaborating elevation-specific growth-climate signals in MXD data. Zhang et al. (2015b) have shown that samples from different elevations with an inhomogeneous temporal distribution may distort the long-term trend

in the final chronology. The sampled high- and low-elevation larch populations have a similar age structure and sample size and reflect two provenances of larch growing within the elevational range from 800–1450 m a.s.l.. However, the absence of substantial inter-site correlations between high- and low-elevation site chronologies as well as mentioned offsets in absolute densities suggest that MXD contains different environmental and climatic signals resulting from habitat differences related to site elevation (Affolter et al., 2010) and bedrock type (Schiller, 1982). These findings are in line with inherent climate signals of TRW measurements from the same sites (Konter et al., 2015a). As a consequence, for climate reconstruction purpose, sites have to be considered separately (Esper et al., 2016).

The strong response to May-June temperatures of trees growing at high-elevation and to March temperatures of trees growing at low-elevation reflects the integrative nature of MXD (Björklund et al.,

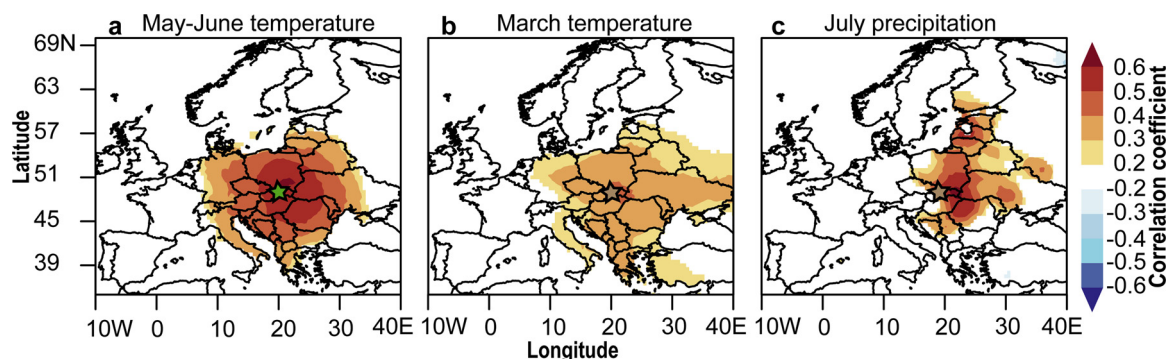


**Fig. 5.** Spatial correlations ( $p < 0.05$ ) between gridded CRU TS 4.01 temperature and precipitation data (1951-2012) and MXD chronologies. a, high-elevation chronologies and May-June temperature, b, low-elevation chronologies and March temperature, and July precipitation. Star indicates the sampling location.

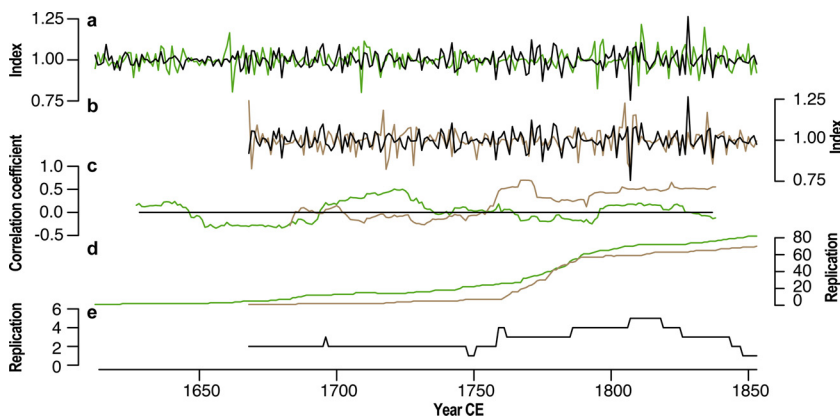


**Fig. 6.** Overlapping period of the MXD historical chronology (black curve) with a, the high-elevation MXD chronology (green), and b, the low-elevation chronology (brown). All chronologies were 10SP detrended. c, 31-year moving window correlations between the chronologies, and d-e, the temporally changing sample replications of the chronologies.

2017), storing environmental information of the whole summer in the cell formation process (Briffa et al., 1998; Büntgen et al., 2017; D'Arrigo et al., 1992). The significant positive association with September temperatures of high-elevation trees indicates the month of growth cessation, because monitoring of the European larch growing season in the central Swiss Alps using micro cores showed that growth at elevations between 1350–2150 m a.s.l. is completed in September (Moser et al., 2010). Despite maximum monthly precipitation sums in the summer month from May to August (Fig. 1), trees at lower elevations are affected negatively by droughts in July. We assume that larch responses to drought as a consequence of raising temperatures (Büntgen et al., 2013), increased evapotranspiration and water-stress caused by growth on well-drained soils developed on limestone rock (Dünisch and Bauch, 1994). Even though positive correlations of temperature sensitive wood density chronologies with August temperature have been widely reported across Europe (Büntgen et al., 2017; Esper et al., 2012; Fuentes et al., 2017; Klippel et al., 2018; Rydval et al., 2017), correlations are not significant in the Tatra, indicating that in the study region climatic conditions in August are of minor importance in the cell development process.

Spatial correlations reveal that the May-June and March temperature signals in high- and low-elevation trees appear at central-eastern European scale, whereas July precipitation signal is spatially limited to a region east of the study side which potentially reflects the higher spatial variability of precipitation (Bacchi and Kottigoda, 1995). In addition, significant differences in the stability of the climate signals between the high- and low-elevation provenance arise by re-calibrating 2000 subset chronologies against monthly climate data. A significant May-June temperature signal preserved in a chronology that contains only five high-elevation MXD series indicates that even with a little sample replication a chronology with a robust climate signal can be composed (Esper et al., 2012). To build a chronology with a stable July precipitation signal however, 20 low-elevation MXD series are needed indicating that despite a stable  $R_{bar}$  value of 0.33 and  $EPS > 0.9$ , which generally exhibit a common variance in a provenance, not all individual trees are July precipitation sensitive. We assume potential micro-site effects (Düthorn et al., 2013) related to differences in soil thickness developed on limestone, modulate the drought sensitivity of single individuals. Trees situated on patches with higher soil availability benefit from its water-holding capacity whereas individuals established on bedrock suffer drought more directly through (rain) water depletion through the fissured rock (Williams et al., 2016; Yang et al., 2014). In addition, we suggest that common variability in the provenance is additionally driven by non-climate factors (Fritts, 1976).

The phenomenon that low-elevation trees respond positively to warm early spring temperatures whereas trees from the same species at a higher altitude respond to summer temperatures has been previously described for Norway spruce TRW series from ten sites in the Tatra Mountains (Savva et al., 2006). Also in Scots pine MXD series from five

sites in the Scandinavian Mountains significant influence of early spring temperatures has been detected (Björklund et al., 2012). However, the positive response of the low-elevation provenance to March temperatures even though cambial activity and xylem cell differentiation processes are not recorded earlier than the month of April in studies from dry inner Alpine valleys (Gruber et al., 2010; Swidrak et al., 2011), climatic and environmental settings that match conditions at the study site, indicates that the signal is not an physically active response of the xylem to climate. Hence, it can be assumed that an increase in spring temperatures may induce earlier snow melt, thereby favoring an earlier stem rehydration and growth onset (Kirilyanov et al., 2003; Vaganov et al., 1999) which positively affects the subsequent stages of cell development.

Negative responses to summer drought and high temperatures of low-elevation provenances and positive responses of high-elevation trees have been reported from the Alps (Hartl-Meier et al., 2014a; Jolly et al., 2005), Eastern Carpathians (Sidor et al., 2015) and Tatra (Büntgen et al., 2007; Savva et al., 2006) and altitudinal growth/climate gradient analysis served as space for time substitute to study the impact of future global warming (Hartl-Meier et al., 2014b). Scots pine from a low-elevation site in the mountain forests south of Poprad has also been used to reconstruct Slovakian drought dynamics over the period 1744–2006 using the Palmer Drought Severity Index (Büntgen et al., 2009). However, we note that despite a significant precipitation signal in the month of July in low-elevation trees, correspondence with regional hydroclimate records including the Slovakian June-August scPSDI reconstruction (Büntgen et al., 2009), a June-August SPI reconstruction from Romania (Levanic et al., 2012) and a scPSDI reconstruction retrieved from the old world drought atlas for the area 19–21E and 48–49.5 N (Cook et al., 2015) is limited with correlation coefficients ranging between 0.19 and 0.34 over the common period of overlap. This also matches the finding that low-elevation trees have certain drought response, but which is not consistent over the whole population.

#### 4.2. Potentials and limitations of the MXD measurements for climate reconstruction

Historical samples were obtained from beams in churches and castles, located in mountain valleys surrounded by the High and Low Tatras, but it is unclear in which sites in the nearby forests the trees were cut (Büntgen et al., 2006a). The range of average MXD values calculated from historical samples support a potential origin from high- and low-elevation sites. Though only an insufficient replication in the period of overlap between historical and living samples is given, the existence of growth consistencies between the low-elevation and historical MXD chronologies, and inconsistencies between these and the high-elevation chronology clearly show that for the successful establishment of a millennium-long MXD chronology with a meaningful and

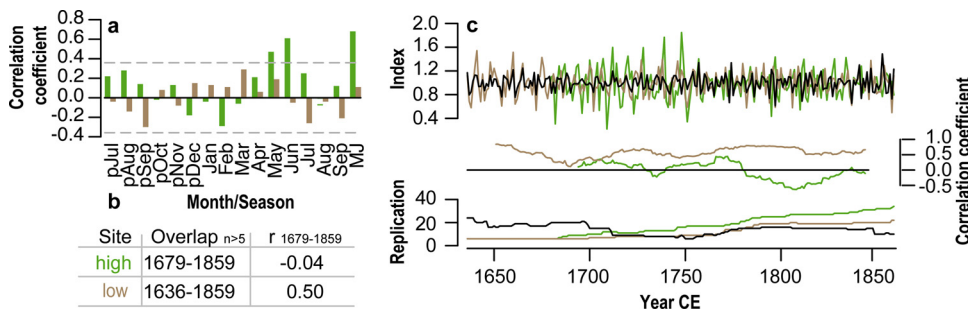


**Fig. 7.** Climate signal and covariance. **a**, Calibration of 10SP high and low-elevation TRW chronologies from the Tatra region published in Büntgen et al. (2013) against monthly and seasonal 10-year HP filtered temperature data from the Poprad station from 1951-2004. Dashed lines approximate  $p < 0.01$  considering the varying lag-1 serial correlations. **b**, Correlation of living-tree site chronologies with the historical chronology from construction wood. **c**, Overlapping period of the historical (black), high-elevation (green) and low-elevation (brown) TRW chronologies, together with the corresponding 31-year moving window correlations and sample replication.

homogenous climate signal through time, the high-elevation trees have to be treated separately (Esper et al., 2016; Tegel et al., 2010). Thus, results clearly indicate that the climatic information preserved in the historical samples is linked to hydroclimate. However, for previous analysis, using TRW to establish a May-June temperature reconstruction (Büntgen et al., 2013), the high-elevation, low-elevation and historical material was merged which indicates (i) substantial differences in the climate signal of MXD and TRW as known from the Mediterranean (Klesse et al., 2015; Seim et al., 2012), or (ii) substantial biases in the TRW reconstruction. Correlation of the MXD 100SP/10SP chronologies with corresponding 100SP/10SP TRW chronologies, retrieved as a byproduct when producing MXD measurements, is  $r = 0.67/0.67$  for the high-elevation and  $r = 0.63/0.57$  for the low-elevation site indicating that direction of the climate signal (positive or negative response with monthly climate data), should be equal in TRW and MXD. Further, re-standardization of high and low-elevation TRW measurements published in Büntgen et al. (2013) (identifier Vernar1 (low) and Tatra (high)) using a 10SP and re-calibration against 10-year high-pass filtered Poprad temperature data clearly indicates that also in TRW the low-elevation trees do not include a substantial May-June temperature signal ( $r = 0.11$ ) which is recorded in high-elevation trees ( $r = 0.68$ ) (Fig. 7a). Similar to MXD, but based on an increased sample replication in TRW, in the period of overlap from 1679 to 1859, historical and low-elevation TRW chronologies show a common variance, whereas a significant correlation with the high-elevation site is absent (Fig. 7b-c). The use of non-temperature sensitive TRW series points to significant bias in the May-June temperature reconstruction which also have been previously illustrated by Konter et al. (2015a). Büntgen et al. (2013) combined trees from seven high- and low-elevation sites, which were scattered over the same area where historical wood samples were derived from, to represent the full ecological range of the natural occurrence of larch in the Tatra region. This sampling strategy lowers site control, and enables to better integrate and date historical samples of unknown origin instead of using one specific provenance within in the ecological range (Büntgen et al., 2011) and has been successfully used to establish tree-ring based proxy reconstructions in central Europe (Büntgen et al., 2011; Scharnweber et al., 2019). However, our findings have shown potential weaknesses of this approach, because the compilation of a master chronology that includes samples from ecological gradients without common variance increases uncertainties the interpretation of preserved climate signals. Further research is required to disentangle climatic signals in the historical in TRW and MXD larch Tatra samples.

## 5. Conclusion

We present an assessment of site-specific climate signals of MXD data in a high- and a low-elevation larch site in the Tatra Mountains, Slovakia. Opposing growth/climate relationships, manifested by a positive influence of warm summers on high-elevation and a positive influence of summer precipitation on low-elevation MXD, indicate that

the living-tree larch sites cannot be merged for climate reconstruction. First tests to connect 56 measurements from historical from the Greater Tatra region, to develop a chronology extending back to 1032 CE indicate that historical data better synchronize with the low-elevation larch chronology, suggesting the climate signal of such a composite MXD chronology would be weighted towards hydroclimate rather than temperatures. We recommend to increase sample replication through the inclusion of additional beams from younger constructions that cover the period of overlap before considering the data for climate reconstructions, especially to further disentangle climate signals preserved in historical samples.

## Declaration of Competing Interest

None.

## Acknowledgements

This research was supported by the German Research Foundation, grants # Inst 247/665-1 FUGG and ES 161/9-1. We thank Markus Kochbeck, Christian Gnanewaran, Eileen Kuhl and Philipp Schulz for producing TRW and MXD measurements, and Valerie Trouet for discussion. The authors declare no conflict of interest.

## Appendix A. Supplementary data

Supplementary material related to this article can be found, in the online version, at doi:<https://doi.org/10.1016/j.dendro.2020.125674>.

## References

- Affolter, P., Büntgen, U., Esper, J., Rigling, A., Weber, P., Luterbacher, J., Frank, D., 2010. Inner Alpine conifer response to 20th century drought swings. *Eur. J. For. Res.* 129, 289–298.
- Bacchi, B., Kottegoda, N.T., 1995. Identification and calibration of spatial correlation patterns of rainfall. *J. Hydrol.* 165, 311–348.
- Barry, R., 2008. Circulation systems related to orography. In: Press, C.U. (Ed.), *Mountain Weather and Climate*, pp. 125–250 Cambridge.
- Björklund, J.A., Gunnarson, B.E., Krusic, P.J., Grudd, H., Josefsson, T., Östlund, L., Linderholm, H.W., 2012. Advances towards improved low-frequency tree-ring reconstructions, using an updated *Pinus sylvestris* L. MXD network from the Scandinavian Mountains. *Theor. Appl. Climatol.* 113, 697–710.
- Björklund, J., Seftigen, K., Schweingruber, F., Fonti, P., von Arx, G., Bryukhanova, M.V., Cuny, H.E., Carrer, M., Castagneri, D., Frank, D.C., 2017. Cell size and wall dimensions drive distinct variability of earlywood and latewood density in Northern Hemisphere conifers. *New Phytol.* 216, 728–740.
- Böhm, R., Jones, P.D., Hiebl, J., Frank, D., Brunetti, M., Maugeri, M., 2009. The early instrumental warm-bias: a solution for long central European temperature series 1760-2007. *Clim. Change* 101, 41–67.
- Briffa, K.R., Jones, P.D., Bartholin, T.S., Eckstein, D., Schweingruber, F.H., Karlen, W., Zetterberg, P., Eronen, M., 1992. Fennoscandian summers from AD 500. Temperature changes on short and long timescales. *Clim. Dyn.* 7, 111–119.
- Briffa, K.R., Schweingruber, F.H., Jones, P.D., Osborn, T.J., Shiyatov, S.G., Vaganov, E.A., 1998. Reduced sensitivity of recent tree-growth to temperature at high northern latitudes. *Nature* 391, 678–682.
- Büntgen, U., Esper, J., Frank, D.C., Nicolussi, K., Schmidhalter, M., 2005. A 1052-year tree-ring proxy for Alpine summer temperatures. *Clim. Dyn.* 25, 141–153.

- Büntgen, U., Frank, D.C., Nievergelt, D., Esper, J., 2006a. 700 years of settlement and building history in the Loetschental, Switzerland. *Erdkunde* 2, 96–112.
- Büntgen, U., Frank, D.C., Nievergelt, D., Esper, J., 2006b. Summer temperature variations in the European Alps, a.d.755–2004. *J. Clim.* 19, 5606–5623.
- Büntgen, U., Frank, D.C., Kaczka, R.J., Verstege, A., Zwijsac-Kozica, T., Esper, J., 2007. Growth responses to climate in a multi-species tree-ring network in the Western Carpathian Tatra Mountains, Poland and Slovakia. *Tree Physiol.* 27, 689–702.
- Büntgen, U., Frank, D., Grudd, H., Esper, J., 2008. Long-term summer temperature variations in the Pyrenees. *Clim. Dyn.* 31, 615–631.
- Büntgen, U., Brázdil, R., Frank, D., Esper, J., 2009. Three centuries of Slovakian drought dynamics. *Clim. Dyn.* 35, 315–329.
- Büntgen, U., Tegel, W., Nicolussi, K., McCormick, M., Frank, D., Trouet, V., Kaplan, J.O., Herzig, F., Heussner, K.U., Wanner, H., Luterbacher, J., Esper, J., 2011. 2500 years of European climate variability and human susceptibility. *Science* 331, 578–582.
- Büntgen, U., Kyncl, T., Ginzler, C., Jaks, D.S., Esper, J., Tegel, W., Heussner, K.U., Kyncl, J., 2013. Filling the Eastern European gap in millennium-long temperature reconstructions. *PNAS* 110, 1773–1778.
- Büntgen, U., Krusic, P.J., Verstege, A., Sangüesa-Barreda, G., Wagner, S., Camarero, J.J., Ljungqvist, F.C., Zorita, E., Oppenheimer, C., Konter, O., Tegel, W., Gärtner, H., Cherubini, P., Reinig, F., Esper, J., 2017. New tree-ring evidence from the pyrenees reveals western Mediterranean climate variability since medieval times. *J. Clim.* 30, 5295–5318.
- Burda, J., Gawęda, A., Klötzli, U., 2013. Geochronology and petrogenesis of granitoid rocks from the Goryczkowa Unit, Tatra Mountains (Central Western Carpathians). *Geologica Carpathica* 64, 419–435.
- Cook, E.R., Krusic, P.J., 2016. Program ARSTAN: a Tree-ring Standardization Program Based on Detrending and Autoregressive Time Series Modeling, Lamont-doherty Earth Observatory. Columbia University, Palisades NY.
- Cook, E.R., Peters, K., 1981. The smoothing spline: a new approach to standardizing forest interior tree-ring width series for dendroclimatic studies. *Tree-Ring Bull.* 41, 45–53.
- Cook, E.R., Peters, K., 1997. Calculating unbiased tree-ring indices for the study of climatic and environmental change. *Holocene* 7, 361–370.
- Cook, E.R., Seager, R., Kushnir, Y., Briffa, K.R., Büntgen, U., Frank, D., Krusic, P.J., Tegel, W., van der Schrier, G., Andreu-Hayles, L., Baillie, M., Baittinger, C., Bleicher, N., Bonde, N., Brown, D., Carrer, M., Cooper, R., Cufar, K., Dittmar, C., Esper, J., Griggs, C., Gunnarson, B., Gunther, B., Gutierrez, E., Haneca, K., Helama, S., Herzig, F., Heussner, K.U., Hofmann, J., Janda, P., Kontic, R., Kose, N., Kyncl, T., Levanić, T., Linderholm, H., Manning, S., Melvin, T.M., Miles, D., Neuwirth, B., Nicolussi, K., Nola, P., Panayotov, M., Popa, I., Rothe, A., Seftigen, K., Seim, A., Svarva, H., Svoboda, M., Thun, T., Timonen, M., Touchan, R., Trotsiuk, V., Trouet, V., Walder, F., Wazny, T., Wilson, R., Zang, C., 2015. Old World megadroughts and pluvials during the Common Era. *Sci. Adv.* 1, e1500561.
- Crutzen, P.J., 2002. Geology of mankind. *Nature* 415, 23.
- D'Arrigo, R.D., Jacoby, G.C., Free, R.M., 1992. Tree-ring width and maximum latewood density at the North American tree line: parameters of climatic change. *Can. J. For. Res.* 22, 1290–1296.
- Dorado Liñán, I., Büntgen, U., González-Rouco, F., Zorita, E., Montávez, J.P., Gómez-Navarro, J.J., Brunet, M., Heinrich, I., Helle, G., Gutiérrez, E., 2012. Estimating 750 years of temperature variations and uncertainties in the Pyrenees by tree-ring reconstructions and climate simulations. *Clim. Past* 8, 919–933.
- Dünisch, O., Bauch, J., 1994. Influence of soil substrate and drought on wood formation of spruce (*Picea abies* [L.] Karst.) under controlled conditions. *Holzforschung* 48, 447–457.
- Düthorn, E., Holzkämper, S., Timonen, M., Esper, J., 2013. Influence of micro-site conditions on tree-ring climate signals and trends in central and northern Sweden. *Trees* 27, 1395–1404.
- Esper, J., Cook, E.R., Krusic, P.J., Peters, K., Schweingruber, F.H., 2003. Tests of the RCS method for preserving low-frequency variability in long tree-ring chronologies. *Tree-Ring Res.* 59, 81–98.
- Esper, J., Büntgen, U., Frank, D.C., Nievergelt, D., Liebhold, A., 2007. 1200 years of regular outbreaks in alpine insects. *Proc. Biol. Sci.* 274, 671–679.
- Esper, J., Büntgen, U., Timonen, M., Frank, D.C., 2012. Variability and extremes of northern Scandinavian summer temperatures over the past two millennia. *Glob. Planet. Change* 88–89, 1–9.
- Esper, J., Büntgen, U., Luterbacher, J., Krusic, P.J., 2013. Testing the hypothesis of post-volcanic missing rings in temperature sensitive dendrochronological data. *Dendrochronologia* 31, 216–222.
- Esper, J., Schneider, L., Smerdon, J.E., Schöne, B.R., Büntgen, U., 2015. Signals and memory in tree-ring width and density data. *Dendrochronologia* 35, 62–70.
- Esper, J., Krusic, P.J., Ljungqvist, F.C., Luterbacher, J., Carrer, M., Cook, E., Davi, N.K., Hartl-Meier, C., Kiryanov, A., Konter, O., Myglan, V., Timonen, M., Treydte, K., Trouet, V., Villalba, R., Yang, B., Büntgen, U., 2016. Ranking of tree-ring based temperature reconstructions of the past millennium. *Quat. Sci. Rev.* 145, 134–151.
- Esper, J., Klippel, L., Krusic, P.J., Konter, O., Raible, C.C., Xoplaki, E., Luterbacher, J., Büntgen, U., 2019. Eastern Mediterranean summer temperatures since 730 CE from Mt. Smolikas tree-ring densities. *Clim. Dyn.* <https://doi.org/10.1007/s00382-019-05063-x>.
- Földvary, G.Z., 1988. *Geology of the Carpathian Region*. World Scientific Publishing, Singapore.
- Frank, D., Esper, J., Cook, E.R., 2007. Adjustment for proxy number and coherence in a large-scale temperature reconstruction. *Geophys. Res. Lett.* 34, L16709. <https://doi.org/10.1029/2007GL030571>.
- Fritts, H.C., 1976. *Tree Rings and Climate*. Blackburn Press, Caldwell, N.J.
- Fuentes, M., Salo, R., Björklund, J., Seftigen, K., Zhang, P., Gunnarson, B., Aravena, J.-C., Linderholm, H.W., 2017. A 970-year-long summer temperature reconstruction from Rogen, west-central Sweden, based on blue intensity from tree rings. *Holocene* 28, 254–266.
- Gawęda, A., 2008. An apatite-rich enclave in the High Tatra granite (Western Carpathians): petrological and geochronological study. *Geologica Carpathica* 59, 95–306.
- Grissino-Mayer, H.D., Fritts, H.C., 1997. The International Tree-Ring Data Bank: an enhanced global database serving the global scientific community. *Holocene* 7, 235–238.
- Gruber, A., Strobl, S., Veit, B., Oberhuber, W., 2010. Impact of drought on the temporal dynamics of wood formation in *Pinus sylvestris*. *Tree Physiol.* 30, 490–501.
- Gunnarson, B.E., Linderholm, H.W., Moberg, A., 2011. Improving a tree-ring reconstruction from west-central Scandinavia: 900 years of warm-season temperatures. *Clim. Dyn.* 36, 97–108.
- Harris, I., 2015. CRU TS3.23: Climatic Research Unit (CRU) Time-Series (TS) Version 3.23 of High Resolution Gridded Data of Month-by-month Variation in Climate (Jan.1901–Dec.2014).
- Hartl-Meier, C., Dittmar, C., Zang, C., Rothe, A., 2014a. Mountain forest growth response to climate change in the Northern Limestone Alps. *Trees* 28, 819–829.
- Hartl-Meier, C., Zang, C., Dittmar, C., Esper, J., Göttele, A., Rothe, A., 2014b. Vulnerability of Norway spruce to climate change in mountain forests of the European Alps. *Clim. Res.* 60, 119–132.
- Hartl-Meier, C., Zang, C., Büntgen, U., Esper, J., Rothe, A., Göttele, A., Dirnbock, T., Treydte, und K., 2015. Uniform climate sensitivity in tree-ring stable isotopes across species and sites in a mid-latitude temperate forest. *Tree Physiol.* 35 (1. Januar), 4–15. <https://doi.org/10.1093/treephys/tpu096>. Nr. 1.
- IPCC, 2018. In: Masson-Delmotte, V., Zhai, P., Pörtner, H.O., Roberts, D., Skea, J., Shukla, P.R., Pirani, A., Moufouma-Okia, W., Péan, C., Pidcock, R., Connors, S., Matthews, J.B.R., Chen, Y., Zhou, X., Gomis, M.I., Lonnoy, E., Maycock, T., Tignor, M., Waterfield, T. (Eds.), *Global Warming of 1.5°C. An IPCC Special Report on the Impacts of Global Warming of 1.5°C Above Pre-Industrial Levels and Related Global Greenhouse Gas Emission Pathways, in the Context of Strengthening the Global Response to the Threat of Climate Change, Sustainable Development, and Efforts to Eradicate Poverty*, In Press.
- Jolly, W.M., Dobbertin, M., Zimmermann, N.E., Reichstein, M., 2005. Divergent vegetation growth responses to the 2003 heat wave in the Swiss Alps. *Geophys. Res. Lett.* 32, L18409. <https://doi.org/10.1029/2005GL023252>.
- Kaczka, R.J., Spyt, B., Janecka, K., Beil, I., Büntgen, U., Scharnweber, T., Nievergelt, D., Wilkming, M., 2018. Different maximum latewood density and blue intensity measurements techniques reveal similar results. *Dendrochronologia* 49, 94–101.
- Kiryanov, A., Hughes, M., Vaganov, E., Schweingruber, F., Silkin, P., 2003. The importance of early summer temperature and date of snow melt for tree growth in the Siberian Subarctic. *Trees* 17, 61–69.
- Klesse, S., Ziehmer, M., Rousakis, G., Trouet, V., Frank, D., 2015. Synoptic drivers of 400 years of summer temperature and precipitation variability on Mt. Olympus, Greece. *Clim. Dyn.* 45, 807–824.
- Klippel, L., Krusic, P.J., Konter, O., St. George, S., Trouet, V., Esper, J., 2018. A 1200+ year reconstruction of temperature extremes for the northeastern Mediterranean region. *Int. J. Climatol.* 39, 2336–2350.
- Konter, O., Rosner, K., Kyncl, Thomas, Esper, J., Büntgen, U., 2015a. Spatiotemporal variations in the climatic response of *Larix decidua* from the Slovakian Tatra Mountains. In: Wilson, R., Helle, G., Gaertner, H. (Eds.), *Proceedings of the DENDROSYMPOSIUM 2014*. Deutsches GeoForschungsZentrum GFZ, pp. 62–69.
- Konter, O., Esper, J., Liebhold, A., Kyncl, T., Schneider, L., Düthorn, E., Büntgen, U., 2015b. Tree-ring evidence for the historical absence of cyclic larch budmoth outbreaks in the Tatra Mountains. *Trees* 29, 809–814.
- Lenz, O., Schär, E., Schweingruber, F.H., 1976. Methodische Probleme bei der radio-graphisch-densitometrischen Bestimmung der Dichte und der Jahringbreiten von Holz. *Holzforschung* 30, 114–123.
- Levanic, T., Popa, I., Poljansek, S., Nechita, C., 2012. A 323-year long reconstruction of drought for SW Romania based on black pine (*Pinus nigra*) tree-ring widths. *Int. J. Biometeorol.* 57, 703–714.
- Linderholm, H.W., Gunnarson, B.E., 2019. Were medieval warm-season temperatures in Jämtland, central Scandinavian Mountains, lower than previously estimated? *Dendrochronologia* 57, 125607. <https://doi.org/10.1016/j.dendro.2019.125607>.
- Melvin, T.M., Grudd, H., Briffa, K.R., 2013. Potential bias in 'updating' tree-ring chronologies using regional curve standardisation: Re-processing 1500 years of Tornetrask density and ring-width data. *Holocene* 23, 364–373.
- Morice, C.P., Kennedy, J.J., Rayner, N.A., Jones, P.D., 2012. Quantifying uncertainties in global and regional temperature change using an ensemble of observational estimates: the HadCRUT4 data set. *J. Geophys. Res.* 117, D08101.
- Moser, L., Fonti, P., Büntgen, U., Esper, J., Luterbacher, J., Franzen, J., Frank, D., 2010. Timing and duration of European larch growing season along altitudinal gradients in the Swiss Alps. *Tree Physiol.* 30, 225–233.
- Niedzwiedz, T., 1992. Climate of the Tatra Mountains. *Mountain Res. Dev.* 12, 131–146.
- Popa, I., Kern, Z., 2009. Long-term summer temperature reconstruction inferred from tree-ring records from the Eastern Carpathians. *Clim. Dyn.* 32, 1107–1117.
- Rydval, M., Loader, N.J., Gunnarson, B.E., Druckenbrod, D.L., Linderholm, H.W., Moreton, S.G., Wood, C.V., Wilson, R., 2017. Reconstructing 800 years of summer temperatures in Scotland from tree rings. *Clim. Dyn.* 49, 2951–2974.
- Savva, Y., Oleksyn, J., Reich, P.B., Tjoelker, M.G., Vaganov, E.A., Modrzynski, J., 2006. Interannual growth response of Norway spruce to climate along an altitudinal gradient in the Tatra Mountains, Poland. *Trees* 20, 735–746.
- Scharnweber, T., Heussner, K.U., Smiljanic, M., Heinrich, I., van der Maaten-Theunissen, M., van der Maaten, E., Struwe, T., Buras, A., Wilkming, M., 2019. Removing the non-analogous bias in modern accelerated tree growth leads to stronger medieval drought. *Sci. Rep.* 9, 2509. <https://doi.org/10.1038/s41598-019-39040-5>.
- Schiller, G., 1982. Significance of bedrock as a site factor for Aleppo pine. *For. Ecol.*

- Manag. 4, 213–223. [https://doi.org/10.1016/0378-1127\(82\)90001-9](https://doi.org/10.1016/0378-1127(82)90001-9).
- Schneider, L., Smerdon, J.E., Büntgen, U., Wilson, R.J.S., Myglan, V.S., Kirilyanov, A.V., Esper, J., 2015. Revising midlatitude summer temperatures back to A.D. 600 based on a wood density network. *Geophys. Res. Lett.* 42, 4556–4562.
- Schweingruber, F.H., Fritts, H.C., Bräker, O.U., Drew, L.G., Schär, E., 1978. The X-Ray technique as applied to dendroclimatology. *Tree-Ring Bull.* 38, 61–91.
- Seim, A., Büntgen, U., Fonti, P., Haska, H., Herzig, F., Tegel, W., Trouet, V., Treyde, K., 2012. Climate sensitivity of a millennium-long pine chronology from Albania. *Clim. Res.* 51, 217–228.
- Sidor, C.G., Popa, I., Vlad, R., Cherubini, P., 2015. Different tree-ring responses of Norway spruce to air temperature across an altitudinal gradient in the Eastern Carpathians (Romania). *Trees* 29, 985–997.
- Swidrak, I., Gruber, A., Kofler, W., Oberhuber, W., 2011. Effects of environmental conditions on onset of xylem growth in *Pinus sylvestris* under drought. *Tree Physiol.* 31, 483–493.
- Tegel, W., Vanmoerkerke, J., Büntgen, U., 2010. Updating historical tree-ring records for climate reconstruction. *Quat. Sci. Rev.* 29, 1957–1959.
- Trouet, V., van Oldenborgh, G.J., 2013. KNMI climate explorer: a web-based research tool for high-resolution paleoclimatology. *Tree-Ring Res.* 69, 3–13.
- Vaganov, E.A., Hughes, M.K., Kirilyanov, A.V., Schweingruber, F.H., Silkin, P.P., 1999. Influence of snowfall and melt timing on tree growth in subarctic Eurasia. *Nature* 400, 149–151.
- Wigley, T., Briffa, K.R., P.D., J., 1984. On the average of correlated time series, with applications in dendroclimatology and hydrometeorology. *J. Clim. Appl. Meteorol.* 23, 201–213.
- Williams, A., Hunter, M.C., Kammerer, M., Kane, D.A., Jordan, N.R., Mortensen, D.A., Smith, R.G., Snapp, S., Davis, A.S., 2016. Soil water holding capacity mitigates downside risk and volatility in US rainfed maize: time to invest in soil organic matter? *PLoS One* 11, e0160974. <https://doi.org/10.1371/journal.pone.0160974>.
- Wilson, R., Anchukaitis, K., Briffa, K.R., Büntgen, U., Cook, E., D'Arrigo, R., Davi, N., Esper, J., Frank, D., Gunnarson, B., Hegerl, G., Helama, S., Klesse, S., Krusic, P.J., Linderholm, H.W., Myglan, V., Osborn, T.J., Rydval, M., Schneider, L., Schurer, A., Wiles, G., Zhang, P., Zorita, E., 2016. Last millennium northern hemisphere summer temperatures from tree rings: part I: the long term context. *Quat. Sci. Rev.* 134, 1–18.
- Yang, F., Zhang, G.-L., Yang, J.-L., Li, D.-C., Zhao, Y.-G., Liu, F., Yang, R.-M., Yang, F., 2014. Organic matter controls of soil water retention in an alpine grassland and its significance for hydrological processes. *J. Hydrol.* 519, 3086–3093. <https://doi.org/10.1016/j.jhydrol.2014.10.054>.
- Zhang, P., Linderholm, H.W., Gunnarson, B.E., Björklund, J., Chen, D., 2015a. 1200 years of warm-season temperature variability in central Fennoscandia inferred from tree-ring density. *Clim. Past* 11, 489–519. <https://doi.org/10.5194/cpd-11-489-2015>.
- Zhang, P., Björklund, J., Linderholm, H.W., 2015b. The influence of elevational differences in absolute maximum density values on regional climate reconstructions. *Trees* 29, 1259–1271. <https://doi.org/10.1007/s00468-015-1205-4>.